THE JOURNAL OF PHYSICAL CHEMISTRY B

Article

pubs.acs.org/JPCB

Release Mechanisms of Poly(ethylene glycol) Macroions from Aqueous Charged Nanodroplets

Jun Kyung Chung and Styliani Consta*

Department of Chemistry, The University of Western Ontario, London, Ontario, Canada N6A 5B7

Supporting Information

ABSTRACT: Ion-release processes in nanodroplets that contain excess charge are of central importance in atmospheric aerosols as well as in determining the charge state distributions of macroions that are detected in electrospray mass spectrometry (ESMS) experiments. We performed molecular simulations of systems of a poly(ethylene glycol) (PEG) associated with various ions (Na^+, Li^+,Ca^{2+}) in aqueous charged nanodroplets in order to investigate the manner that the macroion emerges from an aqueous nanodroplet as well as its final charge state. In the study we focused on a specific region of the parameter space with respect to charge and size of droplets that is close to the Rayleigh limit. We found that for sizes of droplets with linear dimensions of several nanometers and length of PEG up to 100 monomers, the PEG macroion emerges from the droplet following a three-step process: (i) phase separation, (ii) gradual extension of the macroion out of the droplet, and (iii) drying-out of the solvent or spontaneous detachment of the macroion from the droplet. The third step is determined by the ratio of charge on the macroion to the ions in the water portion of the droplet. The chemical transformation that is caused in PEG by the transfer of ions from the solvent into PEG determines its release mechanism. When the charge is carried by macroions, the charge-induced instability manifests by following one of the expected scenarios of Rayleigh instability; however, the assumptions of the Rayleigh model break down. We also examined the release of the macroion below the Rayleigh limit, and we found that the macroion emerges from the droplet by drying-out of the solvent. On balance of phenomenological evidence, we concluded that the ion-evaporation mechanism (IEM) in its most common meaning is not the followed mechanism for the parameter space of the systems that we studied. The final charge state of the macroion is in excellent agreement with the experimental data of Fenn and co-workers.

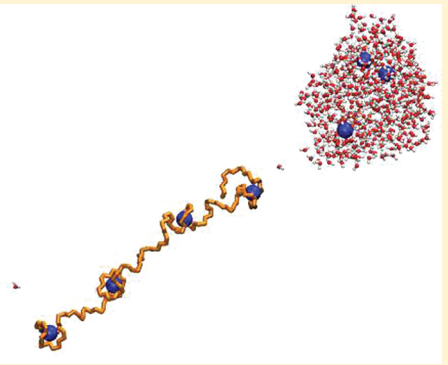

INTRODUCTION

Aqueous nanodroplets with excess charge are ubiquitous in atmospheric aerosols and are also indispensable intermediates in electrospray (ES)[1−8] and liquid jet experiments.[9,10] The charged droplets are composed of solvent and excess ions that may be simple ions such as hydronium ions, alkali ions, or macroions. The analysis of macroions such as proteins and other biological molecules in various charge states has been one of the main usages of electrospray mass spectrometry (ESMS).[2,11,12] In ESMS, these macroions are transferred from the bulk solution into the gaseous state via droplets that contain excess charge. The droplets disintegrate by evaporation of the solvent and fission due to high charge. One of the important questions in ESMS is to identify the factors that determine the charge state distribution of the macroions.[7,13−16] In that respect, the role of the preparation of the sample and spraying conditions[13−15] in the spectrum has been studied. The maximum charge state of a macroion has been also studied by experiments and statistical mechanics modeling.[7,16] Research by Fenn and co-workers[8,17] looked into the relation of the charge state of a macroion to its release mechanism from charged nanodroplets. Our present study is along Fenn's inquiry to relate the release mechanism of macroions to its final charge state. A major stumbling-block in establishing this relation is that the release mechanism cannot be readily detected in experiments when the droplets have linear dimensions in the nanometer range. However, disintegration of highly charged microdroplets may be observed experimentally.[18] Therefore, the evidence for the mechanism in nanodroplets is indirect[19] based on the outcome of wisely chosen experimental systems and conditions.[8]

A simple theoretical model that has often been used to determine the volume to charge ratio for spontaneous fission of a charged droplet is Rayleigh's model.[20] Rayleigh's model is a macroscopic model postulating that the total energy of the charged droplet is the sum of surface energy and electrostatic energy terms. The model further assumes that the droplet has constant volume and uniform electrostatic potential on the surface (the droplet is a conductor). Linear stability analysis with respect to small surface shape fluctuations led to the following criterion that determines the spherical droplet stability:

Received: February 17, 2012
Revised: April 13, 2012
Published: April 24, 2012

dx.doi.org/10.1021/jp301577b | J. Phys. Chem. B 2012, 116, 5777−5785

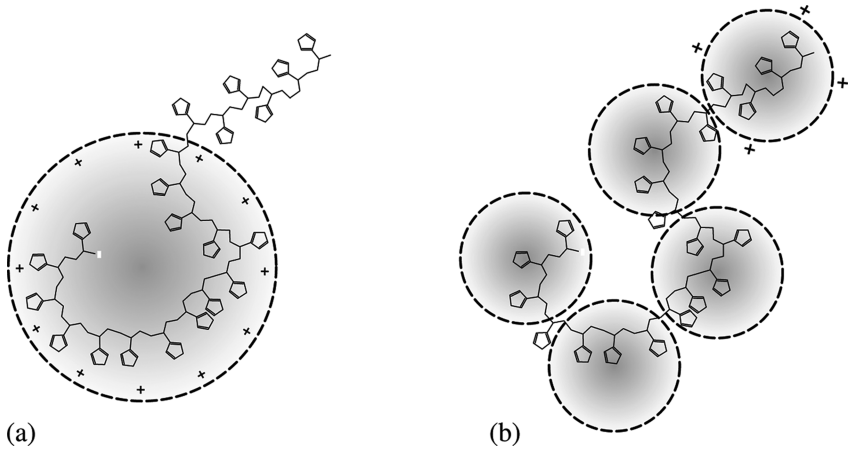

Figure 1. Possible morphology of a droplet that contains a macroion beyond Rayleigh limit. A schematic representation of the solvent distribution around the example of a polyhistidine chain is shown. The dashed circles represent the droplet surface. Induced charge at the droplet surface is indicated on some of the droplet surfaces. (a) Gradual expulsion of the charged segment from the droplet while the remainder of the chain in the droplet has the charge given by the Rayleigh model. The spherical droplet is stable according to the Rayleigh model. (b) Droplet shape consistent with the pearl mechanism of chain collapse.

$$Q^2 = 64\pi^2\sigma\varepsilon_0 R^3 \quad (1)$$

where Q, R, and σ denote the total charge of the droplet, the droplet radius, and the surface tension coefficient, respectively. The effect of simple ions on the stability of the charged droplets has been investigated in computer simulations[21−23] and was found to not significantly affect the criterion for droplet stability.

The Rayleigh mechanism only determines the onset of the instability and not the process in which the instability will reveal itself. In the presence of macroions, there are several scenarios that are consistent with the Rayleigh model and provide extensions for the instability of droplets in the presence of macroions. One plausible scenario is that beyond the Rayleigh limit, the solvent may solvate one charged end of the chain with charge close to Rayleigh limit, while the other end of the chain may protrude like a tail from the droplet by carrying away the rest of the charge. A schematic picture of this plausible scenario is shown in Figure 1a. This scenario is analogous to the way that a droplet that contains single charges fragments at the Rayleigh limit.[22] Another scenario is shown in Figure 1b, where the solvent solvates the charged chain in the form of beads in a necklace. For instance, a system of 1200 water molecules and 20 charges, can form a necklace of beads where every bead contains 200 molecules that solvate five charges in the chain in consistency with the Rayleigh limit. A third scenario of manifestation of Rayleigh instability was found by one of the authors[24] using the example of polyhistidine. In this system, the connectivity of the charge along with the hydrophilic nature of polyhistidine led to the formation of an assembly of spines of highly ordered polar solvent molecules on the surface of the droplet. The surface charge distribution of the spiny droplet is highly nonuniform, and the macroscopic description of the droplet energy as a sum of electrostatic and surface terms is no longer valid. As expected, the validity of all these scenarios will depend on the charge distribution on the chain, the effect of surface tension, and the interplay between solvent−solvent interactions and solvation of the macroions.

In the field of ESMS, the release mechanisms of ions are described by two models: the model of Dole[1] and that of Iribarne−Thomson.[25,26] The former model, which is also called the charge residue model (CRM) proposes that charged droplets fragment by succession of Rayleigh fissions. In these fissions, excess charge carried by simple ions is released. When a macroion is present, it has been suggested that the macroion does not detach from the nanodroplet like the simple ions, but it remains in the droplet where it dries-out.[27] The Iribarne−Thomson model, which is called the ion-evaporation model (IEM), suggests that release of ions may happen in nanodroplets before the Rayleigh limit if the rate of ion evaporation is higher than the solvent evaporation. In this model, the ions are released by an activated process.[21,22,28] The IEM is more difficult to be extended for macroions in droplets. Ion evaporation from a nonsolvated macroion in vacuum was detected in molecular simulations of sodiated poly(ethylene glycol) (PEG).[29]

In this article we use molecular simulations to examine the escape mechanism of a charged PEG macroion from an aqueous nanodroplet and its relation to the final charge state of the macroion. These inquiries are important for understanding the physical and chemical processes that take place in aerosols in general and also in understanding the relation between charge state of macroions and release mechanism from nanodroplets. We modeled aqueous nanodroplets that contained sodiated PEG ions and excess Na^+ ions. To generalize our findings we also performed simulations with Li^+ and Ca^{2+} ions. PEG was chosen for our studies because it has been widely used as an experimental model in ESMS.[17,30−34] PEG of certain length will be indicated hereafter as PEGN, where N is the number of monomers. The present article continues our previous research on charge-induced conformational changes of polyhistidine[24] and PEG macroion in vacuum and of PEG96 in aqueous nanodroplets.[29] Here, we study the release mechanism of PEG macroion by varying the length of the PEG, charge of the droplet, and temperature of the systems.

We found that when aqueous droplets contain charge close to the Rayleigh predicted charge, a PEG associated with ions may emerge out of the droplet in a three-step process: (i) phase separation; (ii) initial gradual extension of the macroion out of the droplet and then (iii) drying-out of the solvent or detachment of the macroion from the droplet. The manner that the macroion will emerge (step iii) depends on the amount

dx.doi.org/10.1021/jp301577b | J. Phys. Chem. B 2012, 116, 5777−5785

of charge that is found on the macroion versus the amount of charge that is left in the water portion of the droplet. We found that droplets with charge close to the Rayleigh limit emit PEG54-4Na^+, while PEG96-7Na^+, PEG96-7Li^+, and PEG96-3Ca^{2+} emerge by drying-out of the solvent. By performing a number of computational tests, we concluded that the detachment of PEG54−4Na^+ does not follow the IEM mechanism but rather fission due to charge instability. Differences between the Rayleigh model and the found mechanism are identified. To our knowledge, detachment of a nonsolvated macroion from a water nanodroplet is reported for the first time in the literature. Regardless of the manner of release, we found that the droplet environment plays a critical role in the charging of the macroion. We compared the computational data for the charge state of the released PEG with the experimental data of Fenn and co-workers,[17] and the results are in excellent agreement. We also revisited a proposed analytical model by Fenn that led to the suggestion that charged PEG is released by the IEM mechanism. We revised the model and found that, differently from the suggested mechanism, the macroions are released in approximately their maximum charge state.

MODEL AND COMPUTATIONAL METHODS

Computer modeling of PEG54-*n*Na^+, PEG96-*n*Na^+, PEG96-*n*Li^+, and PEG96-*n*Ca^{2+} in aqueous nanodroplets was carried out using DL_POLY[35−37] molecular simulation program. The systems were found in vacuum without any periodic boundary conditions. The PEG molecules were modeled by the OPLS united atom force field.[38] This force field includes Coulomb interactions between partial charges assigned on the atomic sites, Lennard-Jones (LJ) interactions between the various atomic sites, and torsional interactions, as well as angle and bonding interactions modeled by harmonic spring potential functions. The partial charges and LJ parameters are presented in Table 1. Nonbonded interaction parameters for ion−ion

Table 1. Parameters of LJ Potential $4\varepsilon[(\sigma/r)^{12} - (\sigma/r)^6]$ and Partial Charges

atom type	ε (kcal/mol)	σ (Å)	charge (e)
H at chain end	0.0	0.0	0.435
O at chain end	0.170	3.070	−0.7
CH_2 at chain end	0.118	3.905	0.265
CH_2	0.118	3.8	0.25
O	0.170	3.0	−0.5
Na^+	0.003	3.33	1.0
Li^+	0.01828	2.1265	1.0
Ca^{2+}	0.44966	2.4120	2.0

interactions in water were taken from Aqvist.[39] The ion−water site cross-site interactions were found using the combining rules for the ε and σ values of the LJ potential function: $\varepsilon_{ij} = (\varepsilon_i\varepsilon_j)^{1/2}$ and $\sigma_{ij} = (\sigma_i\sigma_j)^{1/2}$. The water molecules were represented by the extended simple point charge (SPC)[40] with flexible angle and bonds in order to capture salient features of surface tension.[41] All the above-described forces were taken into account explicitly without imposing any distance cutoffs. All the snapshots presented here were generated by using the molecular visualization software VMD.[42]

Preparation of Initial Configurations. Initial configurations were prepared by placing shells of 900 and 800 water molecules around a compact conformation of previously equilibrated PEG54-3Na^+ and PEG96-4Na^+, respectively.[29] The majority of simulations were performed by randomly placing six and seven additional Na^+ ions in the water shell containing PEG96-4Na^+ and PEG54-3Na^+, respectively. Simulations were also performed with fewer Na^+ in the water portion of the nanodroplets. Before PEG54-3Na^+ and PEG96-4Na^+ were placed in the aqueous droplet, they had been equilibrated in vacuum[29] by using constant-temperature molecular dynamics (MD) simulations at T = 300 K for 0.6 μs with a Nosé−Hoover thermostat.[43,44] The time step of those simulations was 1 fs. The reason that the charge states of PEG54-3Na^+ and PEG96-4Na^+ were selected as initial configurations is as follows. From the data presented in ref 17, it was estimated that in the initial bulk solution the concentration of Na^+ was approximately 100 times larger than that of PEG. In our previous research,[29] we studied the solvation of sodiated PEG, and we found that the Na^+ ions have a high tendency to be solvated by the ethylene oxide modules of PEG in droplets of PEG−water−Na^+. Given the concentrations of PEG and Na^+ in bulk solution, we would expect that PEG would have at least one or more Na^+ attached to it. The concentration of Na^+ increases substantially in the droplet environment relative to the bulk, and therefore the chemical equilibrium would shift toward further sodiation of PEG. PEG54-3Na^+ and PEG96-4Na^+ were selected as natural starting configurations in the small nanodroplets, where the macroions have not attained yet the maximum charge state and maximum hydrophobicity. Had we started the simulations with PEG54-Na^+ (or PEG96-Na^+), the equilibration could have taken much longer. For other initial charge states of PEG, we would expect the same outcome as with PEG54-3Na^+ (and PEG96-4Na^+) if the solvent evaporation were mild.

Determining the Charge of the Droplets. The number of water molecules included in the droplet was guided by the requirement to have droplets with approximate radius 2−3 nm with overall charge slightly below or close to the Rayleigh limit. The surface tension (σ) of the nanodroplet was treated in the following way: We observed that the water−PEG nanodroplets are not uniform; therefore, we cannot define the surface tension for those systems. However, since we found out that sodiated PEG−water nanodroplets phase separate, we may consider applying the Rayleigh criterion into the two subsystems. In our previous study,[29] we found that for nonsolvated PEG54 and PEG96, the Rayleigh limit is close to 3 Na^+ and 4 Na^+, respectively. This result was based on the population profiles of various conformations characterized by order parameters and not on an a priori assumption about the surface tension. Critical charge (Rayleigh limit) for nonsolvated PEGs in vacuum was defined as the charge where the sodiated PEG populates both globular and extended conformations with equal probability. These conformations are in dynamic equilibrium. Since the value of the charge that leads to equal population probabilities between globular and extended states may be a fractional number, which is unphysical, we found the closest integral charge (3 Na^+ and 4 Na^+ for PEG54 and PEG96, respectively) to the critical charge of the chains. Regarding the water portion, for 800−900 water-molecule nanodroplets, the Rayleigh's criterion (eq 1) yields critical charges of 7−8 e when the surface tension of bulk water (71.97 mN/m) is used. However, even if we were to apply the Rayleigh criterion using surface tension values for bulk water−PEG mixtures[45] in the range of 44.23−70.17 mN/m (depending on PEG concentration and length), the critical charge is found to be in the range of 9−11e.

dx.doi.org/10.1021/jp301577b | J. Phys. Chem. B 2012, 116, 5777−5785

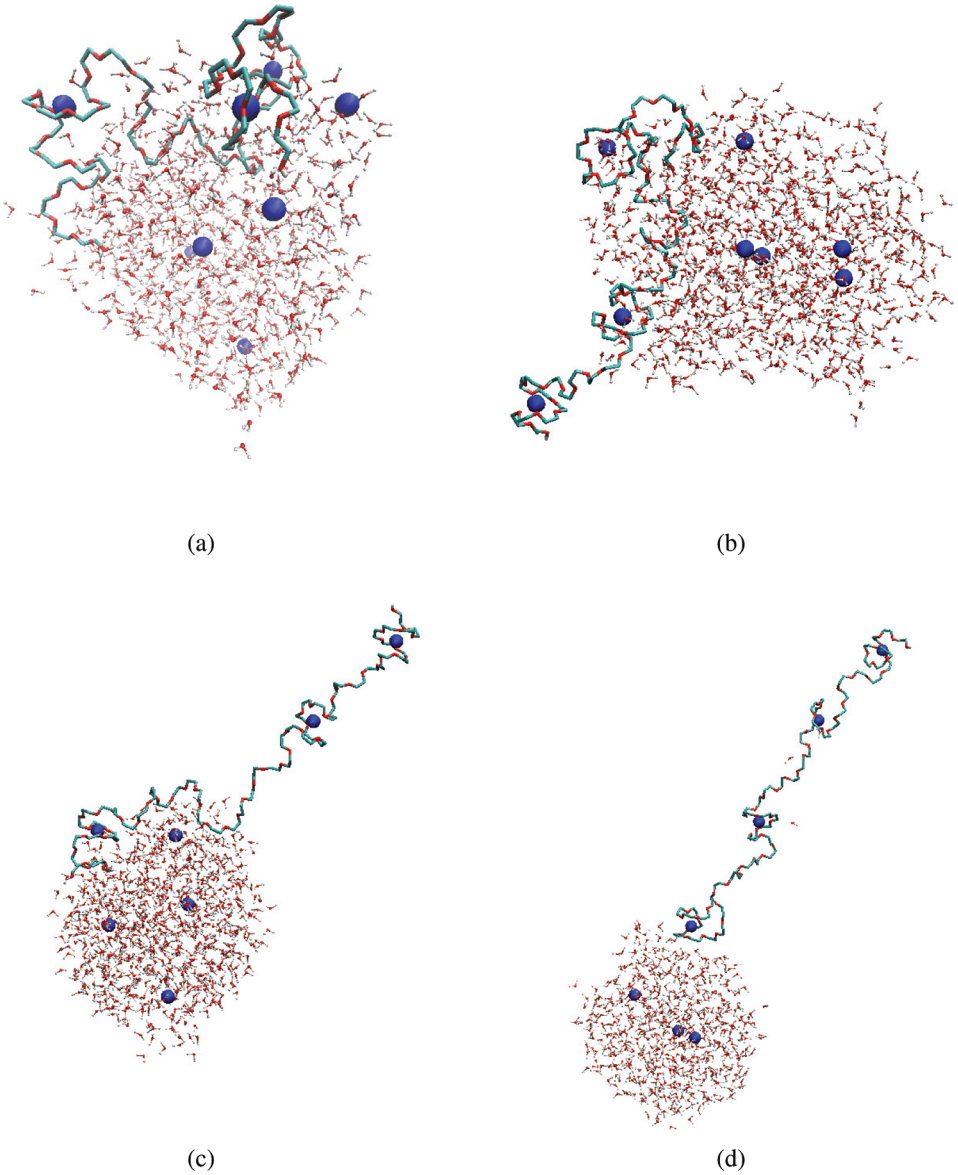

Figure 2. Release of sodiated PEG54 at T = 300 K from droplet that contains initially 900 H_2O, PEG54-3Na^+, and 7 Na^+ ions in the water. (a) PEG54-3Na^+ in a droplet that contains 841 H_2O after evaporation in t = 3 ns; (b) at t = 3.5 ns, part of the PEG54-3Na^+ extends out of the droplet; c) at t = 8 ns, the system contains 747 H_2O, and the portion of PEG that extends out of the droplet gets larger as time passes; (d) at t = 25.15 ns, just before the PEG54-4Na^+ escapes from the droplet. About 580 water molecules have remained in the droplet.

In this approach, we found the volume of the entire nanodroplet used in eq 1 by the volume of the nanodroplets from simulations. In conclusion, both approximate methods to find the critical charge for the sizes of the systems that we study give values in the range of 9−11 e.

Equilibration. Once the initial configurations of the systems were prepared, the total potential energy was minimized at very low temperature. Then, the systems were thermalized by Nosé−Hoover[43,44] MD, and simulations were performed at 300, 350, and 400 K. The time step of the simulations was 1 fs. We examined temperatures of a solute (PEG) and solvent molecules separately and found that no separate thermostatting was needed. Every 2 ns, the evaporated water molecules and ions were removed from the system. A molecule was considered evaporated if it was 80 Å or more away from the center of mass of PEG at the end of each 2 ns period. The release of the macroion from the droplet was completed in approximately 25 ns for sodiated PEG54. For sodiated PEG96, the evaporation time was longer.

Similar simulations to those with Na^+ were also performed for PEG96 with Li^+ and Ca^{2+} ions. Summary of the realizations that were performed at various temperatures are presented in the Supporting Information.

RESULTS AND DISCUSSION

A common feature in all simulations of PEG54-3Na^+ and PEG96-4Na^+ at the various temperatures and number of Na^+ ions as well as in PEG96 with Li^+ and Ca^{2+} ions is that, initially, the charged PEG phase separates from the aqueous nanodroplet because of its reduced hydrophilicity once it is charged.[46] Typical snapshots of the solvated PEG54-3Na^+ and its release mechanism at T = 300 K are shown in Figure 2 for a system that contains 900 water molecules and 7 Na^+ ions in the water portion. Figure 2a shows that PEG54-3Na^+ lies on

dx.doi.org/10.1021/jp301577b | J. Phys. Chem. B 2012, 116, 5777−5785

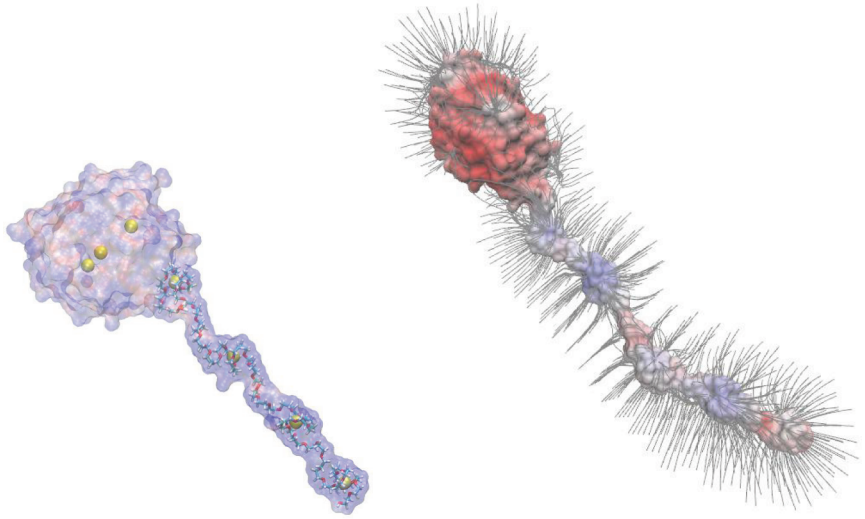

(a) (b)

Figure 3. Electrostatic potential in the presence of PEG macromolecules. (a) Distribution of electrostatic potential on the vdW surface of the droplet. The values of the potential in units of unit charge over Å are shown using a red−white−blue color map. The values of the potential range from 0.3 Z/Å (red) to 0.4 Z/Å (blue) (see text). (b) Electrostatic field lines in the vicinity of the charged droplet−macromolecule system.

the interface between vacuum-droplet with a radius of gyration (R_g) of approximately 1.2 nm. This conformation is different from the bare PEG54-3Na $^+$ in vacuum[29] that was found to make frequent transitions between compact and extended conformation with R_g in the range of 0.4−1.2 nm. In these transitions, the compact form (R_g = 0.4 nm) was more preferable. In Figure 2b,c, the gradual extension of the PEG54-3Na$^+$ from the droplet is shown. In Figure 2c, PEG54-3Na$^+$ is near a state to become PEG54-4Na$^+$. The fourth Na$^+$ ion diffuses in the droplet by lying intermittently in the interior and surface, with preference to the surface. The diffusion of Na$^+$ ions is assisted by the shape fluctuations of the droplet. Figure 2d shows the release of PEG54-4Na$^+$. At this stage, PEG54-4Na$^+$ lingers with the one end in contact with the droplet, until it is finally detached.

To examine further the charge distribution on the surface, the electrostatic potential on the van der Waals (vdW) surface of the droplet was analyzed. The potential was computed using the PBEQ module of the CHARMM molecular modeling package[47] using a linear grid spacing of 1.4 Å. The variance of the electrostatic potential on the vdW surface was then calculated and plotted using a molecular graphics program. In Figure 3a we display the electrostatic potential on the vdW surface of a droplet composed of 587 water molecules, PEG54, and seven sodium ions. Rayleigh's model predictions are based on the assumption of the existence of mobile charges and, as a consequence, uniform electrostatic potential on the surface of the droplet. In the presence of PEG macromolecules, this assumption breaks down in the course of spherical droplet evolution. The main reason for this is the strong noncovalent binding of the PEG molecule and sodium ions and reduced mobility of the charges. Nevertheless, the variations in the potential 0.3−0.4 Z/Å are orders of magnitude smaller than the corresponding variance of a potential induced by a point charge of +7 e on the equivalent surface. Since in this system the Rayleigh model may break down, hereafter the term Rayleigh fission is used in a more general manner meaning instability induced by the high charge of the system. In Figure 3b, electrostatic field lines are plotted in the vicinity of PEG96 macromolecule doped with sodium cations. Inspection of the plot demonstrates that the field lines are orthogonal to the main chain of the macromolecule (i.e., $\nabla\phi\cdot\vec{l} = 0$, where ϕ and $\vec{l}$ are the electrostatic potential and the direction of the chain, respectively). Were the field not orthogonal to the main chain, there would be resulting migration of the charge along the chain. This result is the consequence of higher charge lability along the chain and the aforementioned binding of the cations to the PEG molecule.

Realizations were also performed by starting with the configuration shown in Figure 2d with one and two Na$^+$ ions in the water portion instead of three. It was found that PEG54-4Na$^+$ returned to the droplet and then dried-out. During the process, PEG54-4Na$^+$ did not extend out of the droplet but laid on the surface. The fact that PEG54-4Na$^+$ returned to the droplet showed that the aqueous systems of PEG54-4Na$^+$ with one and two Na$^+$ ions in the water portion are below the Rayleigh limit.

The release mechanism of PEG54-3Na$^+$ was also examined at T = 400 K and was found to be the same as that at 300 K. Well below the Rayleigh limit, PEG54-3Na$^+$ in a droplet of 900 water molecules and 4 Na$^+$ ions showed a drying-out mechanism at both 300 and 400 K. The various processes were examined with four other initial conditions, and the outcomes were the same with respect to the charging mechanism.

For PEG96-7Na$^+$, the release mechanism has the same physical and chemical origin as the release of PEG54-4Na$^+$; however, it has different features[29] from that of PEG54-4Na$^+$. Instead of detaching, PEG96-7Na$^+$ emerged by extending out of the droplet and finally drying-out the solvent. Initial configurations of PEG96-4Na$^+$ in droplets of 800 water molecules containing 6 Na$^+$ ions at T = 350 K readily became PEG96-7Na$^+$. The first five segments of PEG that contain Na$^+$ extended out of the droplet spontaneously at the initial stage of the evaporation process. Two sodiated segments remained attached to the water portion that contained one or none Na$^+$ (the Na$^+$ ions had escaped or attached to PEG). These segments stayed close to the water due to weak vdW interactions and weak electrostatic interactions of the PEG

dx.doi.org/10.1021/jp301577b | J. Phys. Chem. B 2012, 116, 5777−5785

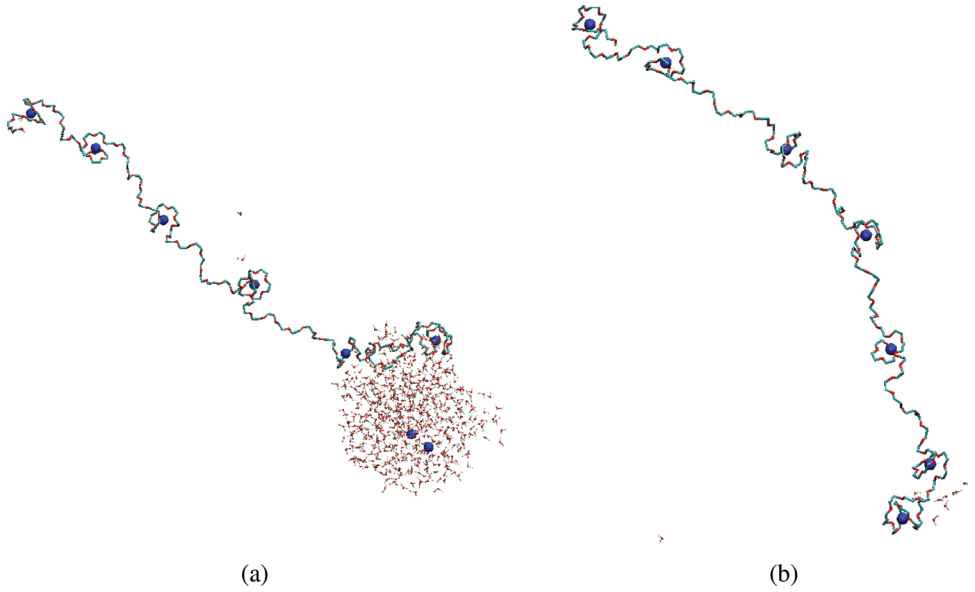

Figure 4. Last stages of the release of sodiated PEG96 by drying-out of the solvent at T = 350 K.

sites with the water molecules. The final stages of drying out are shown in Figure 4. The difference in the release mechanisms between PEG96-7Na^+ and PEG54-4Na^+ is explained as follows: We have reported[24] that one of the ways of manifestation of Rayleigh instability for macroions in a droplet is by the expulsion of the chain from the droplet in a similar manner as the expulsion of a single ion from the droplet by the formation of bottle-necked configurations.[21,22] The manner in which PEG54-4Na^+ and PEG96-7Na^+ are released follows this mechanism. In PEG96−7Na^+, the chain is long enough to hold enough charge that it is released from the droplet by the extension of PEG96-7Na^+ out of the droplet. In the last stage of drying out, there is only one Na^+ ion left in the water portion of approximately 150 water molecules, while another Na^+ ion is attached to the end of PEG that is sunk in the water. One Na^+ ion in water is not sufficient to expel the chain out of the water portion. In PEG54-4Na^+, the chain is short enough to detach from the droplet since there are sufficient Na^+ ions that remain in the water portion of the droplet to repel out the chain. However, at temperatures high enough for Na^+ ions to evaporate, drying-out of the shorter chain may also be observed.

In systems with initial conditions of 800 H_2O, PEG96-4Na^+ and six extra Na^+ ions in the water portion at T = 400 K, PEG96-7Na^+ or PEG96-6Na^+ was formed, which eventually dried-out. Out of six initial conditions, PEG96-6Na^+ was formed in two of the realizations. The lower charge state of PEG is observed because the rate of escape of solvated Na^+ ion may be higher than the rate of sodiation of PEG96.

To understand how general the drying-out mechanism is, we examined aqueous droplets with PEG96 charged with Li^+ and Ca^{2+} ions. The drying-out process was also found for these systems. However, the way that the water molecules are distributed along the chain is different: in PEG charged with Li^+, the chain extends out of the droplet as in PEG with Na^+ ions (see Supporting Information) but in PEG charged with Ca^{2+} ions, the water molecules form large clusters that solvate the regions of PEG that contain the Ca^{2+} ions (see Supporting Information).

In summary, our simulations showed that chemical changes in the charging of macromolecules such as changes in their degree of hydrophilicity play a critical role in determining their mechanisms of release out of the aqueous nanodroplets. In the course of droplet decrease, the charge density of the droplet steadily increases as $[Q] \sim 1/(\text{volume})^{1/2}$ (eq 1). This increase in the charge density leads to the shift of chemical equilibrium toward highly sodiated states of PEG. This critical step of chemical transformation of the macromolecule determines the charge state of PEG and also its release mechanism. The role of the chemical transformation is not captured in both the Rayleigh and IEM models. Both models are macroscopic and take into account the role of the solvent in terms of surface tension and dielectric constant. We found that in aqueous nanodroplets with charge close to the Rayleigh limit, long PEG macroions extend out of the droplet, and finally they emerge by drying-out of the solvent. Short macroions are detached from the droplet once they extend out. The critical step of charging of the macroion leads to its release in droplets that contain charge close to the Rayleigh limit. On the basis of the Rayleigh limit, a charged macroscopic droplet will split into two macroscopic droplets determined by spherical shape deformation along the l = 2 mode. In the simulations we found that the Rayleigh instability manifests itself through contiguous chain extrusion rather than droplet fission. The dramatically different picture of the escape found in the simulations is attributed to the breakdown of several assumptions implicit in the stability analysis. Rayleigh's model predictions are based on the assumption of the existence of mobile charges and, as a consequence, uniform electrostatic potential on the surface of the droplet. In the presence of PEG macromolecules, this assumption breaks down in the course of spherical droplet evolution. The main reason for this is the strong noncovalent binding of the PEG molecule and sodium ions and reduced mobility of the charges.

In comparison to IEM, we found that, contrary to the picture of a fast activated event of single ion escape in IEM, we observed a contiguous extrusion process coupled to droplet evaporation. The aforementioned coupling to the solvent evaporation and the fact that the onset of the extrusion

dx.doi.org/10.1021/jp301577b | J. Phys. Chem. B 2012, 116, 5777−5785

happened at the droplet charge close to the Rayleigh limit indicate that the extrusion is a manifestation of the Rayleigh instability in the presence of charged macromolecules. On balance of phenomenological evidence, we concluded that IEM in its most common meaning is not readily applicable here.

Below the Rayleigh limit, where it is possible to encounter the IEM, we also found drying-out of the macroions, but IEM might be still valid for the evaporation of the solvated Na^+ ions with water or ethylene oxide modules. Depending on the temperature, the competition between the rate of evaporation of solvated Na^+ ions and sodiation of the PEG chain will affect the charge state by producing macroions with lower charge than what is possibly the maximum charge state of sodiated PEG (the maximum charge state is discussed in the following paragraphs).

Model of the Maximum Charge of the Chain. To validate our findings, the charge state of the released sodiated PEG is compared with the experimental findings of Fenn and co-workers[17] shown in Figure 5. For chains up to 100 monomers, the data of Fenn and simulations fall on the same straight line. The agreement between experimental data and simulations validates the realistic nature of our computational model. Simulations show that up to 100 monomers, the distribution of Na^+ ions on the chain is one Na^+ ion per 13.6 monomers. The deviation of the experimental data from the straight line becomes slightly larger for PEG chains of approximately 200 and 400 monomers. It is noted that in the same article Fenn and co-workers developed an intuitive analytical model to estimate the maximum charge a PEG may hold. Unlike proteins in which the composition may be nonuniform along the chain, PEG is a linear homopolymer; therefore, it is amenable to modeling its maximum charge state. Fenn's[17] model is based on the simple assumption that the maximum charge is held by PEG when the binding energy of the central charge equals the repulsive energy from neighboring positive charges in the chain. Additional assumptions that were made in ref 17 for the model and the modifications based on the simulation findings are

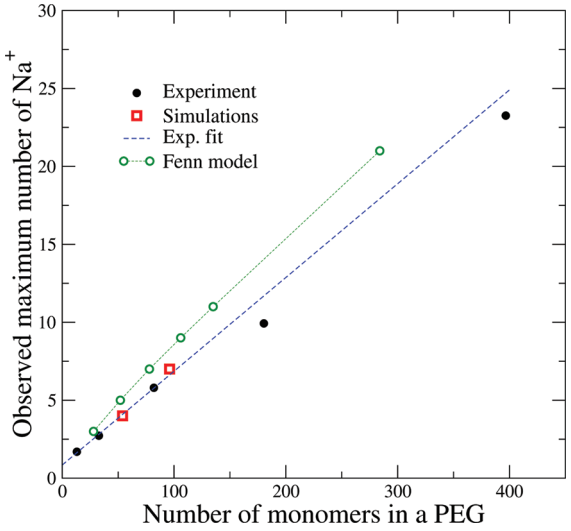

Figure 5. Maximum number of Na^+ ions attached to PEG found in experiments of Wong et al.[17] (black dots) and current simulations (red squares). The green circles represent data using the revised model of Fenn. The straight blue and green lines are included for guiding the eye.

(i) On PEG, the bonding sites are the oxygen atoms. In ref 17, the number of sites was taken to be $s + 1$, where s is the number of ethylene oxide modules in PEG and the additional site comes from the −OH that attaches to the free carbon bond at the end of the PEG. In our simulations we did not find Na^+ attached to the −OH sites of PEG.

(ii) In ref 17, it was considered that the PEG molecule has a linear zigzag configuration with a distance L between sites of 3.5 Å. In our simulation we found the value of L to be in the range of 2.35−2.45 Å .

(iii) In ref 17, the distribution of the n charges on a PEG molecule was considered to be such that the end sites are occupied and the remaining charges are on sites that are as nearly equidistant from each other as possible. We found that the end −OH's are not occupied, and the locations of ions are almost uniform along the chain.

(iv) In ref 17, the energy (E) of the central charge in electronvolts is taken to be the pairwise sum over all other charges of terms comprising A/x, where x is the distance between the charges, and A is the Coulomb constant for unit charges in appropriate units. In our simulations, the binding energy was found by the Coulomb interactions between Na^+ and oxygen as well as methylene sites using the partial charges in Table 1 and distances estimated from radial distribution profiles.

Based on the assumptions in ref 17, the proposed model reads:

$$E = \left[\frac{2A(n-1)}{sL}\right]\left[\frac{1}{n} + \sum_{i=1}^{(n-2)/2} 1/i\right] \quad (2)$$

when n is an even number. When n is odd, the $1/n$ term within the second set of brackets is omitted, and the upper limit for the summation becomes $(n-1)/2$.

From eq 2 it follows that

$$s = \left[\frac{2A(n-1)}{gL}\right]\left[\frac{1}{n} + \sum_{i=1}^{(n-2)/2} 1/i\right] \quad (3)$$

where g is the bonding energy between the charge and the oxygen atom site, and s is the number of ethylene oxide modules in the PEG. It was also assumed that g between the PEG and Na^+ is about the same as the bonding energy of 2.05 eV between Na^+ and dimethoxyethane.

Even though the basic assumption is reasonable, at the time when the model was developed, there were no simulation data to show a realistic structure of charged PEG. As a result, the ions were placed at equal distance on the PEG without considering the coordination of the ions by the monomers. The radial distribution functions of our simulations show that each Na^+ is coordinated by eight oxygen sites of the ethylene oxide monomers arranged in a helix surrounding Na^+. Subsequently, this complex is surrounded by 17 methylene groups. In that way, the +1 e charge of sodium is transferred away from its center. By this correction, the model may be modified in the distance x between Na^+ ions. $x = sL/(n-1)$, becomes $x = (sL - 8nL)/(n-1)$, where L is the length of the monomer, s is the number of monomers in the chain, n is the number of charges, and 8 is the average number of monomers that participate in the coordination of Na^+. The value of L is also changed from 3.5 Å to 2.35−2.45 Å . The binding energy is found by the

dx.doi.org/10.1021/jp301577b | J. Phys. Chem. B 2012, 116, 5777−5785

Coulomb interactions considering the parameters in Table 1 used in our molecular modeling.

Fenn's initial model overestimates by almost twice the experimental and thus our simulation data. Since the assumptions of the model were reasonable, Fenn suggested that the detected state of PEG may be unsaturated in charge and concluded that this is an indication that PEG is released by the IEM mechanism. In view of our data about the structure of sodiated PEG, we revised Fenn's model, and the new data are also presented in Figure 5. For chains up to approximately 100 monomers, the difference between the revised model, simulations, and experiments are within one Na^+ ion, so as we can say that when PEG leaves the droplet, it contains charge close to its maximum capacity. Another reason for the difference between the model and the experimental data is that the PEG chain is not straight, but it has a wavy configuration that brings the Na^+ ions closer; therefore, fewer Na^+ ions may be held by the chain. Most likely this is not an important effect, especially in shorter chains.

CONCLUSION

In this study, we examined the release mechanism of PEG associated with ions (Na^+, Li^+, Ca^{2+}) from charged aqueous nanodroplets. We performed simulations with charge and size of droplet parameters that are close to the Rayleigh limit. We found that for sizes of droplets with linear dimensions of several nanometers and length of PEG up to 100 monomers, the PEG macroion emerges from the droplet following a three-step process: (i) phase separation, (ii) contiguous extension of the macroion out of the droplet, and (iii) drying-out of the solvent or spontaneous detachment of the macroion from the droplet. The third step is determined by the ratio of charge on the macroion to the ions in the water portion of the droplet. Estimates of the potential energy inside the droplets indicate that the reduced mobility of the charges show variations in the electrostatic potential contrary to the steady potential assumed by Rayleigh's model. Since the variations are not very large relative to the variations that are produced by an immobile single point high charge ion, one may say that there is a degree of deviation from Rayleigh's assumptions. We found that the length of the chain and temperature play an important role in the way that the macroion emerges from the droplet. In droplets below the Rayleigh limit, the PEG macroions dried out. IEM is described by an activated process that involves a rare fluctuation that leads the system to the barrier top of the free energy profile. Once the system reaches the barrier top, the escape of the ion should take place rapidly. In simulations we did not find escape of macroion below the Rayleigh limit, but rather a contiguous extrusion process coupled to droplet evaporation. On the basis of phenomenological evidence, we conclude that IEM in its most common meaning is not readily applicable here.

The manner in which PEG54-$n$$Na^+$ and PEG96-$n$$Na^+$ emerge from the droplet is different from the mechanism that was found for a multiply charged polyhistidine in a water droplet.[24] In the charged polyhistidine−water system, the macroion lies entirely in the interior of the droplet. In the Rayleigh instability regime, the water molecules form spines that distribute the charge in space and evaporation of water or other ions becomes scarce. This kind of manifestation of Rayleigh instability cannot be described by a model that considers the energy of the droplet as the sum of electrostatic energy and surface energy. The different mechanisms of release of macroions in the typical cases of polyhistidine and charged PEG that we studied is attributed to the degree of hydrophilicity of the macroion.

In terms of ES experiments, our findings may be related to the behavior of nanodroplets when the evaporation of the solvent occurs slowly once they leave the Taylor cone. Our findings were consistent for the expulsion of a charged PEG with various ions from an aqueous nanodroplet and other hydrophobic ions. More caution is needed in generalizing our conclusions for the release of proteins from nanodroplets under realistic experimental conditions that contain protons. Proteins depending on their degree of hydrophilicity may follow a drying-out mechanism or emission of the macroion similar to that of the PEG with ions. However, the presence of hydronium ions instead of Na^+ ions and the occurrence of electrochemical processes in ES may change the chemistry of the droplets and, therefore, the way that the proteins are expelled from a droplet.

ASSOCIATED CONTENT

Supporting Information

Part of the movies of the drying out process for PEG96-7Na^+, PEG96-4Li^+, and PEG96-3Ca^{2+} are presented. Summary of the realizations are included. This material is available free of charge via the Internet at http://pubs.acs.org.

AUTHOR INFORMATION

Corresponding Author

*E-mail: styliani.constas@gmail.com.

Notes

The authors declare no competing financial interest.

ACKNOWLEDGMENTS

S.C. thanks the Discovery Grant of Natural Sciences and Engineering Research Council of Canada (NSERC) for funding this research and SHARC-Net for providing the computing facilities to perform the simulations.

REFERENCES

(1) Dole, M.; Mack, L.; Hines, R.; Mobley, R.; Ferguson, L.; Alice, M. *J. Chem. Phys.* **1968**, *49*, 2240−2249.
(2) Kebarle, P.; Verkerk, U. H. *Mass Spectrom. Rev.* **2009**, *28*, 898−917.
(3) Segev, E.; Wyttenbach, T.; Bowers, M. T.; Gerber, R. B. *Phys. Chem. Chem. Phys.* **2008**, *10*, 3077−3081.
(4) Wyttenbach, T.; Bowers, M. T. *Annu. Rev. Phys. Chem.* **2007**, *58*, 511−533.
(5) de la Mora, J. F.; Thomson, B. A.; Gamero-Castano, M. *J. Am. Soc. Mass Spectrom.* **2005**, *16*, 717−732.
(6) Williams, E. *J. Mass Spectrom.* **1996**, *31*, 831−842.
(7) Schnier, P.; Gross, D.; Williams, E. *J. Am. Soc. Mass Spectrom.* **1995**, *6*, 1086−1097.
(8) Nguyen, S.; Fenn, J. B. *Proc. Natl. Acad. Sci. U.S.A.* **2007**, *144*, 1111−1117.
(9) Eggers, J. *Rev. Mod. Phys.* **1997**, *69*, 865−929.
(10) Yarin, A. L.; Koombhongse, S.; Reneker, D. H. *J. Appl. Phys.* **2001**, *90*, 4836−4846.
(11) Wyttenbach, T.; Bowers, M. T. *J. Phys. Chem. B* **2011**, *115*, 12266−12275.
(12) Flick, T. G.; Merenbloom, S. I.; Williams, E. R. *Anal. Chem.* **2011**, *83*, 2210−2014.
(13) Hewavitharana, A. K.; Herath, H. M. D. R.; Shaw, P. N.; Cabot, P. J.; Kebarle, P. *Rapid Commun. Mass Spectrom.* **2010**, *24*, 3510−3514.
(14) Verkerk, U.; Peschke, M.; Kebarle, P. *J. Mass Spectrom.* **2003**, *38*, 618−631.

(15) Felitsyn, N.; Peschke, M.; Kebarle, P. *Int. J. Mass Spectrom.* **2002**, *219*, 39−62.
(16) Iavarone, A. T.; Williams, E. R. *J. Am. Chem. Soc.* **2003**, *125*, 2319−2327.
(17) Wong, S. F.; Meng, C. K.; Fenn, J. B. *J. Phys. Chem.* **1988**, *92*, 546−550.
(18) Gomez, A.; Tang, K. Q. *Phys. Fluids* **1994**, *6*, 404−414.
(19) Kebarle, P.; Tang, K. *Anal. Chem.* **1993**, *22*, 972−986.
(20) Rayleigh, Lord *Philos. Mag.* **1882**, *14*, 184.
(21) Consta, S. *J. Mol. Struct.* **2002**, *591*, 131−140.
(22) Consta, S.; Mainer, K.; Novak, W. *J. Chem. Phys.* **2003**, *119*, 10125−10132.
(23) Ichiki, K.; Consta, S. *J. Phys. Chem. B* **2006**, *110*, 19168−19175.
(24) Consta, S. *J. Phys. Chem. B* **2010**, *114*, 5263−5268.
(25) Iribarne, J.; Thomson, B. *J. Chem. Phys.* **1976**, *64*, 2287−2294.
(26) Thomson, B.; Iribarne, J. *J. Chem. Phys.* **1979**, *71*, 4451−4463.
(27) de la Mora, J. F. *Anal. Chim. Acta* **2000**, *406*, 93−104.
(28) Labowsky, M.; Fenn, J. B.; de la Mora, J. F. *Anal. Chim. Acta* **2000**, *406*, 105−118.
(29) Consta, S.; Chung, J. K. *J. Phys. Chem. B* **2011**, *115*, 10447−10455.
(30) Robinson, E. W.; Garcia, D. E.; Leib, R. D.; Williams, E. R. *Anal. Chem.* **2006**, *78*, 2190−2198.
(31) Ude, S.; de la Mora, J. F.; Thomson, B. A. *J. Am. Chem. Soc.* **2004**, *126*, 12184−12190.
(32) Nohmi, T.; Fenn, J. *J. Am. Chem. Soc.* **1992**, *114*, 3241−3246.
(33) Nasibulin, A. G.; de la Mora, J. F.; Kauppinent, E. I. *J. Phys. Chem. A* **2008**, *112*, 1133−1138.
(34) Larriba, C.; de la Mora, J. F. *J. Phys. Chem. B* **2012**, *116*, 593−598.
(35) Smith, W.; Yong, C. W.; Rodger, P. M. *Mol. Simul.* **2002**, *28*, 385−471.
(36) Smith, W.; Forester, T.; Todorov, I. T. *The DL_POLY_2.0 User Manual*; Daresbury Laboratory: Cheshire, U.K., 2009.
(37) http://www.ccp5.ac.uk/DL_POLY/.
(38) Jorgensen, W. L.; Tirado-Rives, J. *J. Am. Chem. Soc.* **1988**, *110*, 1657−1666.
(39) Aqvist, J. *J. Phys. Chem.* **1990**, *94*, 8021−8024.
(40) Brendsen, H. J. C.; Postma, J. P.; van Gunsteren, W. F.; Hermans, J. In *Intermolecular Forces*; Pullman, B., Ed.; Springer: New York, 1981; pp 331−342.
(41) Alejandre, J.; Tildesley, D. J.; Chapela, G. A. *J. Chem. Phys.* **1995**, *102*, 4574−4583.
(42) Humphrey, W.; Dalke, A.; Schulten, K. *J. Mol. Graphics* **1996**, *14.1*, 33−38.
(43) Nosé, S. *Mol. Phys.* **1984**, *52*, 255−268.
(44) Hoover, W. G. *Phys. Rev. A* **1985**, *31*, 1695−1697.
(45) Kim, M. W. *Colloids Surf., A* **1997**, *128*, 145−154.
(46) Rogers, R. D.; Jezl, M. L.; Bauer, C. B. *Inorg. Chem.* **1994**, *33*, 5682−5692.
(47) Brooks, B.; Bruccoleri, R.; Olafson, B.; States, D.; Swaminathan, S.; Karplus, M. *J. Comput. Chem.* **1983**, *4*, 187−217.